An anti-diffusive VOF method for simulation of free surface wave over a bump

Y. G. Chen, W. G. Price and P. Temarel

Ship Science, School of Engineering Sciences, University of Southampton,
Southampton SO17 1BJ, UK

Email: y.chen@soton.ac.uk

1. Introduction

In the fields of naval architecture and ocean engineering there has been an increasing interest on the coupled gas/liquid flow. The liquid sloshing in partially filled LNG tanks, violent water wave impact on ships such as air entrainment by breaking bow waves and slamming, wind/wave interactions, hull skin friction reduction by micro-bubbles and air layer, are examples where the influences of air/gas are not negligible. In order to better understand air's role, a coupled air/water two phase flow model is necessary.

In this investigation, an unsteady Navier–Stokes solver for incompressible two-fluid flows is coupled with an anti-diffusive VOF method to simulate free surface flow over a bump. The two-fluid flow of air and water is approximated by a continuous interface method where the motion equations governing both air and water flow are written in a single fluid formulation and fluid properties, such as density and viscosity, change across the interface. The advantages of the continuous interface method, mainly, are that the surface tension effect can be easily considered by adding a body force to the momentum equations, and furthermore, no special treatment is needed at the interface.

2. Governing Equations

For the free surface flows investigated, air and water are both assumed to be incompressible and immiscible. The resulting equations of motion for the system are governed by the following Navier-Stokes equations

$$\frac{\partial u_j}{\partial x_j} = 0, \tag{1}$$

$$\rho\frac{\partial u_i}{\partial t} = -\frac{\partial}{\partial x_j}(\delta_{ij}p) - \rho\frac{\partial}{\partial x_j}(u_i u_j) + \frac{\partial}{\partial x_j}[\frac{\mu}{\mathrm{Re}}(\frac{\partial u_i}{\partial x_j} + \frac{\partial u_j}{\partial x_i})] - \frac{\rho g_i}{\mathrm{Fr}^2}, \tag{2}$$

where the repeated index implies summation. The coordinates x_i, velocity components u_i and accelerations g_i are non-dimensionalized for each specific problem in terms of a characteristic length L, a characteristic velocity U_0 and gravitational acceleration g. The fluid density ρ and viscosity μ are non-dimensionalised by the corresponding water parameters ρ_w and μ_w, time t by L/U_0 and pressure p by $\rho_w U_0^2$. Re and Fr denote Reynolds and Froude numbers, respectively, and are defined as $\mathrm{Re} = LU_0/\nu_w$, $\mathrm{Fr} = U_0/\sqrt{Lg}$.

The dynamic condition at the interface is automatically implemented via solving equations (1) and (2). In this study the kinematic boundary condition is imposed by means of the VOF method. The interface is convected by the following advection equation

$$\frac{\partial C}{\partial t} + u_i\frac{\partial C}{\partial x_i} = -\gamma\, C(1-C)u_3, \tag{3}$$

where the scalar function C is the volume fraction of a cell occupied by a particular fluid.

In equation (3) we introduce an artificial damping term on the right hand side of equation (3) to avoid wave reflections on the domain boundaries. $u_3 = w$ is the vertical component of velocity and γ is the strength of damping which is non-zero only near the computational boundaries (inlet and outlet).

Using the above volume fraction function C, we can define the corresponding smoothed density ρ and viscosity μ functions based on a simple volume average as (index *a* denotes air)

$$\rho = (1-C)\rho_a / \rho_w + C\,, \tag{4}$$

$$\mu = (1-C)\mu_a / \mu_w + C\,. \tag{5}$$

The details of the numerical method can be found in previous publications in which a level set method is used to capture free surface wave [1, 2].

3. An anti-diffusive VOF method for interface capturing

Equation (3), used to evolve the interface, is an advection equation. In order to reduce numerical diffusion, normally, a complicated geometrical reconstruction of an interface is needed to evaluate the net flux flowing out of each cell. It is noted that upwind schemes are numerically stable but smear the interface due to numerical diffusion, whereas downwind schemes, although numerically unstable, have the advantage of keeping sharp interfaces. In our recent investigation, an anti-diffusive VOF method was introduced by combining a first-order limited downwind scheme with higher order accurate ENO schemes [3]. Here we omit the detailed derivation process and briefly describe the numerical method.

Corresponding to equation (3), we first consider the linear scalar conservation law expressible in the one-dimensional form

$$\frac{\partial C}{\partial t} + u\frac{\partial C}{\partial x} = 0\,. \tag{6}$$

We assume a uniform spatial grid, $x_j = j\Delta x$, and equation (6) is discretized by a finite volume or finite difference method given by

$$\overline{C}_j^{n+1} = \overline{C}_j^{n} - \lambda u(\hat{C}^n_{j+\frac{1}{2}} - \hat{C}^n_{j-\frac{1}{2}}) = 0. \tag{7}$$

Here $\overline{C}_j^n = \dfrac{1}{\Delta x}\displaystyle\int_{x_{j-\frac{1}{2}}}^{x_{j+\frac{1}{2}}} C(x,t^n)$ is the approximation at the n-*th* time step to the cell average of $C(x,t)$, $\lambda = \dfrac{\Delta t}{\Delta x}$ and $\hat{C}^n_{j+\frac{1}{2}}$ is the numerical flux at the cell interface. For the sake of simplicity, we will omit superscript index *n* and denote by $\overline{C}_j^{new}$ the updated value $\overline{C}_j^{n+1}$ in equation (7).

The first-order limited downwind scheme for sharpening contact discontinuities used in [4] constructs a conditional downwind scheme which is nonlinearly stable in the sense that it satisfies the maximum principle and total variation diminishing (TVD) property. When the anti-diffusive limited downwind scheme is applied to equation (7), the numerical flux $\hat{C}^n_{j+\frac{1}{2}}$ in equation (7) can be explicitly expressed as

$$\hat{C}^{anti}_{j+\frac{1}{2}} = \hat{C}^{diss}_{j+\frac{1}{2}} + \text{minmod}(\hat{C}^{l}_{j+\frac{1}{2}} - \hat{C}^{diss}_{j+\frac{1}{2}}, \hat{C}^{r}_{j+\frac{1}{2}} - \hat{C}^{diss}_{j+\frac{1}{2}})\,, \tag{8}$$

where the dissipative flux $\hat{C}^{diss}_{j+\frac{1}{2}}$ is the classical upwind flux, and $\hat{C}^{l}_{j+\frac{1}{2}}$ and $\hat{C}^{r}_{j+\frac{1}{2}}$ are the extremal left-wind and right-wind fluxes. They are respectively defined as

$$\hat{C}^{diss}_{j+\frac{1}{2}} = \overline{C}_{j+1}\,,\ \hat{C}^{l}_{j+\frac{1}{2}} = \overline{C}_{j}\,,\ \hat{C}^{r}_{j+\frac{1}{2}} = \frac{\overline{C}_{j+2} - \overline{C}_{j+1}}{\lambda u} + \overline{C}_{j+2} \text{ for } u < 0\,, \tag{9}$$

$$\hat{C}^{diss}_{j+\frac{1}{2}} = \overline{C}_{j}\,,\ \hat{C}^{l}_{j+\frac{1}{2}} = \frac{\overline{C}_{j} - \overline{C}_{j-1}}{\lambda u} + \overline{C}_{j-1}\,,\ \hat{C}^{r}_{j+\frac{1}{2}} = \overline{C}_{j+1} \text{ for } u > 0\,. \tag{10}$$

In equation (8) the minmod function is defined as

$$\text{minmod}(b,\ c) = \begin{cases} 0 & bc \le 0, \\ b & bc > 0, |b| \le |c|, \\ c & bc > 0, |c| < |b|. \end{cases} \tag{11}$$

The scheme expressed in equation (7) with the limited downwind flux defined in equation (8) has the important feature of keeping its shape for all time for a single travelling discontinuity under the CFL condition $\lambda|u| \le 1$.

The simplest way to construct a second order accurate scheme is to replace the piecewise constant cell average $\overline{C}_j$ in equation (7) by conservative, non-oscillatory, piecewise linear functions

$$C_j(x) = \overline{C}_j + \text{minmod}\left(\frac{\overline{C}_{j+1} - \overline{C}_j}{\Delta x}, \frac{\overline{C}_j - \overline{C}_{j-1}}{\Delta x}\right)(x - x_j),$$

$$x \in I_j = [x_{j-\frac{1}{2}}, x_{j+\frac{1}{2}}],\ \forall j. \tag{12}$$

By applying equation (12) to equation (8) we derive a second order limited downwind scheme expressible in the compact form

$$\hat{C}^{anti}_{j+\frac{1}{2}} = \hat{C}^{+}_{j+\frac{1}{2}} + \text{minmod}\left(\frac{\overline{C}_{j+2} - \overline{C}_{j+1}}{\lambda u} + \hat{C}^{+}_{j+\frac{3}{2}} - \hat{C}^{+}_{j+\frac{1}{2}}, \hat{C}^{-}_{j+\frac{1}{2}} - \hat{C}^{+}_{j+\frac{1}{2}}\right) \text{ for } u < 0, \tag{13}$$

$$\hat{C}^{anti}_{j+\frac{1}{2}} = \hat{C}^{-}_{j+\frac{1}{2}} + \text{minmod}\left(\frac{\overline{C}_{j} - \overline{C}_{j-1}}{\lambda u} + \hat{C}^{-}_{j-\frac{1}{2}} - \hat{C}^{-}_{j+\frac{1}{2}}, \hat{C}^{+}_{j+\frac{1}{2}} - \hat{C}^{-}_{j+\frac{1}{2}}\right) \text{ for } u > 0, \tag{14}$$

where the interface fluxes $\hat{C}^{+}_{j+\frac{1}{2}}$ and $\hat{C}^{-}_{j+\frac{1}{2}}$ at $x = x_{j+\frac{1}{2}}$ are defined by

$$\hat{C}^{+}_{j+\frac{1}{2}} = C_{j+1}(x_{j+\frac{1}{2}}),\ \hat{C}^{-}_{j+\frac{1}{2}} = C_j(x_{j+\frac{1}{2}}). \tag{15}$$

The interested readers can refer to previous work for the details of multi-dimensional extension [3].

4. Numerical results

The numerical model presented here is used for simulating regular wave generated by a submerged bump on a horizontal bottom, which has been investigated numerically by Huang et al [5] and experimentally by Cahouet [6]. The obstacle has a polynomial shape defined by

$$h(x) = \frac{27}{4} E \frac{x}{L}\left(\frac{x}{L} - 1\right)^2 \qquad (0 \le x \le L),$$

where L is the length of the bump and E=0.1L. One supercritical case (Fr=1.0) and two subcritical cases (Fr=0.426 and 0.304) were selected to validate the numerical method.

The air/water ratios of density and viscosity are specified as $1.2\text{x}10^{-3}$ and $1.8\text{x}10^{-2}$, respectively. The computational domain extends from $-8.0 \le x/L \le 15.0$ and $-H/L \le z/L \le 0.5$ for all three test cases. The physical parameters and computational mesh resolutions are given in table.

Table: Computational conditions for the 2D steady-state flow over a submerged bump

	$Fr = U_0/\sqrt{Lg}$	$\text{Re} = LU_0/\nu_w$	H/L	Mesh resolution
Case1	1.0	$8.52\text{x}10^{+5}$	0.228	211x121
Case2	0.426	$3.63\text{x}10^{+5}$	0.670	281x281
Case3	0.304	$3.00\text{x}10^{+5}$	0.500	281x251

Since we focus on validation of free surface capturing method and are not interested in the details of flow near the bump in this study, slip boundary condition is imposed on the bump surface and bottom, and only laminar flow is solved for all cases studied here. At t=0 a uniform velocity u=1.0 is set and computation was terminated after a steady-state solution was reached for each case. Figure 1 shows a comparison of wave profile with experimental data for three cases. Figure 2 presents velocity vector and iso-lines for fluid volume fraction C=0.05, 0.5 and 0.95 for case 1, where for the sake of clarity velocities are plotted in a smaller area over the bump. For case 1 the wave profile shows good agreement with measurement as can be seen in Fig. 1(A), whereas the calculated wave crest by Huang et al [5] is lower than the experimental data. The waves after the first crest obtained by both numerical methods are damped out quickly for case 3.

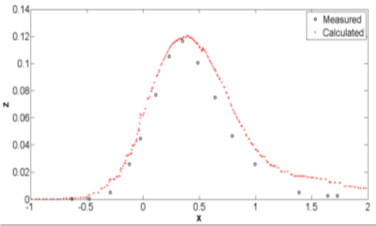

(A) Case 1

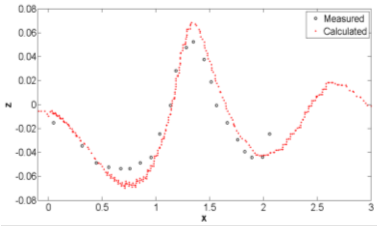

(B) Case 2

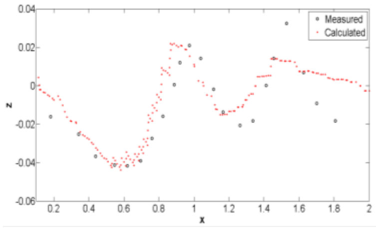

(C) Case 3

Figure 1 Comparison of calculated wave elevation with measured data for each case (where x and z are non-dimensionalised by L)

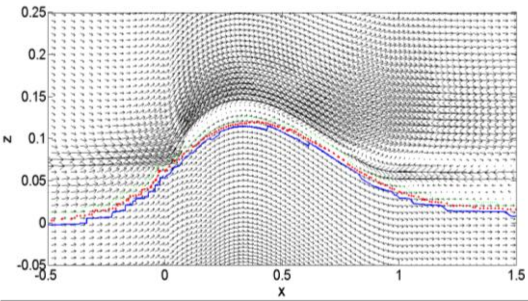

Fig. 2 Velocity vector and iso-lines of fluid volume fraction C=0.05, 0.5 and 0.95 (from top to bottom) for case 1

5. Conclusions

An anti-diffusive VOF method was developed and implemented in a continuous two-fluid model for the computation of free surface waves. The present method proved to be robust and gives reasonably good results compared to experimental measurements and other available numerical methods.

Acknowledgements

The authors would like to acknowledge the support of The Lloyd's Register Educational Trust, through its University Technology Centre at the University of Southampton.

Reference

1. Price, W. G., and Chen, Y. G. (2006). "A simulation of free surface waves for incompressible two-phase flows using a curvilinear level set formulation," Int. J. Numer. Meth. Fluids 51, pp305-330.
2. Chen, Y. G., Djidjeli, K. and Price, W. G. (2009). "Numerical simulation of liquid sloshing phenomena in partially filled containers," Comput. Fluids 38, pp830-842.
3. Chen Y. G., Price, W. G. and Temarel, P. (2010). "An anti-diffusive volume of fluid method for interfacial fluid flows," International Journal for Numerical Methods in Fluids. In press.
4. Despres B. and Lagoutiere, F. (2001). "Contact discontinuity capturing schemes for linear advection, compressible gas dynamics," Journal of Scientific Computing 16: 479-524.
5. Huang J., Carrica P. M. and Stern F. (2007). "Coupled Ghost Fluid/Two-Phase Level Set Method for Curvilinear Body-Fitted Grids," International Journal for Numerical Methods in Fluids, Vol. 55, pp. 867-897.
6. Cahouet J. (1984). "Etude Numerique er Experimentale du Probleme Bidimensionnel de la Resistance de Vagues Non-Lineaire," PhD thesis**,** ENSTA, Paris (in French).